

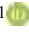




Influence of Three Different Wavy Walls on Nanofluid Flow over a Double Forward Facing Step in the Presence of Circular Cylinders Cross-Section Arrays

Sarah H. Ali¹, Sarah Rabeea Nashee^{2*}, Marwah Yousif Jalil¹

¹ University of Sumer, Thi-Qar 64005, Iraq

² Department of Mechanical Engineering, College of Engineering, University of Thi-Qar, Thi-Qar 64001, Iraq

Corresponding Author Email: sara.rabee@utq.edu.iq

Copyright: ©2025 The authors. This article is published by IETA and is licensed under the CC BY 4.0 license (<http://creativecommons.org/licenses/by/4.0/>).

<https://doi.org/10.18280/ijht.430437>

ABSTRACT

Received: 7 July 2025

Revised: 18 August 2025

Accepted: 25 August 2025

Available online: 31 August 2025

Keywords:

double forward-facing step, nanofluid, circular cylinders cross-section, corrugated wall, overall performance

For fluid behavior and heat transfer examinations, a double forward-facing step design is a classic example. It is beneficial to benchmarking because it is good characterized. In this paper, a particular forward facing step flow heat transmission situation ($Re = 5000-35000$) is investigated using computational fluid dynamics. When added to a water-based fluid, Al_2O_3 nanoparticles are thought to create nanofluids with varying volumetric concentrations (0, 2, 4, 6%). A forward-facing step is passed by laminar flow. Three examples of wavy lower walls—triangular, square, and sinusoidal—were employed in the study with the presence of three array of circular cylinders cross-section at the entrance before the steps. Every upper surface that tested has adiabatic properties. The lower surface has a constant surface temperature. The simulation findings indicate that a reattachment point and a separation bubble follow a forward-facing step. Due to physical interference, the upper's corrugated surfaces create a different. In the presence of nanofluid, sectional to warm of the channel presents an intriguing heat flux. Heat transport and parameters have a pseudo-linear relationship. As flow velocity and nanoparticle concentrations rise, thermal convection naturally rises as well. Re number has a significant impact on heat flux and, consequently, Nusselt number because of the drastic changes in flow structure. Additionally, there is a clear correlation between increased convection and nanoparticle concentration. Additionally, by improving heat transfer through the vortices it creates, the corrugated top layer has a physical influence. The best heat transfer and thermal performance are provided by triangular corrugated surface cases ($\eta = 1.76$). then the square ($\eta = 1.67$), and at last, the sinusoidal ($\eta = 1.53$), all this obtained by applied 6% volumetric concentrations of the nanoparticles.

1. INTRODUCTION

Many academics find a forward-facing step channel flow to be an intriguing subject since it incorporates the separation and reattachment processes. A sharp expansion or contraction in the geometries, such as backward-forward facing steps, causes the flow to separate and then rejoin. Numerous engineering applications, including combustion chambers, environmental management mechanisms, electronic equipment cooling systems, highly efficient heat exchangers, cooling sections in wind turbine blades and chemistry, and energy system equipment, are influenced by this phenomenon. As a consequence, a considerable mixing of both high and lowest energy occurs in the reattachment zone. It is at the upper acute corner of the step that the backward-facing step separates, creating a recirculating area behind the step [1-3].

For enhancing the thermal and hydrodynamic performance of thermal systems in general and of step-forward channels in particular, engineers and researchers are compelled to create more efficient energy systems in order to facilitate the effective utilization of energy sources due to the increasing use of energy sources over time. In order to increase the rate of

heat transfer with a manageable pressure drop, the researchers carried out numerous studies. Making more compact heat exchangers, which are used in air conditioning systems, nuclear reactors, heat exchangers, thermal power plants, chemical reactors, and numerous thermal applications, can be greatly aided by that [4-6].

Wavy walls are frequently employed in a variety of technical applications, including heat exchanges, electronic device cooling, and serpentine cooling air channels for gas turbine internal cooling. To achieve the intended heat transfer in various applications, the separation zone's strength and size must be controlled. Even if the geometry is straight forward, the problem nonetheless has a complicated flow field. To gain a better understanding, more work involving the examination of some modifications to the given geometry is therefore required. Many studies have been evaluated in relation to forward-facing channels in addition to the circular cylinder cross-section which in turn applied in mechanical engineering, cylindrical structures like (cables, rods, pipes, and fibers etc.) that frequently used in applications such as acoustic wave units and ultrasonic nondestructive assessment methods. In terms of acoustic utilizations, mechanistic modeling of wave

propagation through cylinders is crucial for comprehending the operation of these particular structures and is beneficial for their overall design. Isotropic cylinders are the main focus of early research on elastic oscillation propagation in cylindrical waveguides [7, 8].

Furthermore, over the last ten years, a novel method for enhancing heat transmission by introducing ultra-fine solid particles into fluids has been widely applied. In contrast to typical particles (millimeter or micro-scale), the particles remain suspended in the fluid and do not sediment, which results in an increase in the pressure drop in the flow field. Thus, employing nanofluids to improve heat transfer in isolated areas is highly beneficial. Increasing the convective heat transfer coefficient, also known as the Nusselt number, in separated flows is how this improvement is achieved [9-11].

Thermal performance improvement has served as the foundation for both experimental and numerical study. These studies unequivocally demonstrated that corrugated flow channels are one of the most effective means of increasing the rate of heat transfer [12, 13]. The use of wavy creates a very complicated flow pattern that encourages improved momentum transfer and flow recirculation, which raises the rate of heat transmission [14, 15]. Laminar flow with convection over horizontal, vertical, and sloped, forward- and backward-facing steps channel was experimentally studied by He et al. [16]. It was discovered that adding stairs that face both forward and backward intensifies the velocity's turbulence and variations in temperature downstream of the step. The findings also show that, under comparable flow and temperature circumstances, the greatest local Nusselt number is almost twice as high for the backward-facing step and three times higher for the forward-facing step than for the flat plate value. The longitudinally of the Re numbers for backward-facing step flow between 450 and 1050 was investigated by Barkley et al. [17].

Kherbeet et al. [18] experimentally examined how the heat transfer properties were affected by nanofluid flow over forward-facing and backward-facing steps. The range of the Reynolds number was 280–480. The SiO₂ nanoparticle concentrations were 0.005 and 0.01. According to the experimental findings, the greatest Nusselt number was recorded at the concentration of 1% H₂O–SiO₂ nanofluid. The contrast between MBFS and MFFS demonstrated that utilizing the forward-facing step yields the highest Nusselt number.

Also, Kherbeet et al. [19] recently used a finite volume method to numerically analyze the flow of nanofluids along a micro scale forward-facing step. Different kinds of nanoparticles, including (SiO₂, Al₂O₃, and CuO) were distributed in an ethylene glycol base fluid with a volume fraction ranging from 0 to 0.04. According to the findings, the SiO₂ nanofluid had the greatest Nusselt number. The other finding is that when the density of the nanoparticle material decreases, the diameter of the nanoparticles decreases, and the volume fraction increases, the Nusselt number rises.

A numerical research on heat transfer and nanofluid flow across a backward-facing step was published by Abu-Nada [20]. The nanoparticles have a variety of Re numbers between 200 and 600 and volume fractions between 0.05 and 0.2. Effective areas with high heat conductivity outside of the recirculation zones were also found by the analysis. Moreover, a numerical investigation on laminar five distinct nanoparticles added to water moving in abrupt expansion was conducted by Christopher et al. [21]. The backward-facing

flow and abrupt expansion flow with Reynolds numbers ranging from 30 to 150 were solved using the same technique as Kanna and Das [22] at nanoparticles volume fraction (0.1, 0.2, and 0.05). In comparison to Abu-Nada's [20] data, the results showed a reduction in the reattachment length of about 1.3%.

Nie and Armaly [23] used a Laser-Doppler Velocimeter (LDV) to measure the variation in velocity and the reattachment duration on a 3-dimension flow following of a backward facing step. The findings investigate how the separation length varies with different flow and Reynolds numbers, which were identified by the separation length fluctuation. An experimental study on the recirculation zone formed downstream of a forward-facing step sinking in the turbulent boundary layer was conducted by Sherry et al. [24]. Here, the factors influencing the boundary layer's turbulent mixing, velocity deficit, and technique disrupting the reattachment area were identified and discussed. Over forward facing step, Li et al. [25] looked at disturbed turbulent flow. They noted an improvement in local heat transmission and a shorter recirculation bubble.

This work presents a novel configuration by combining three important elements: (1) the use of three different wavy lower wall geometries (triangular, square, and sinusoidal) chosen for their different effects on vortex formation and boundary layer disruption; (2) the addition of a three-row array of circular cylinders upstream of the steps, which improves flow mixing and thermal boundary layer thinning; and (3) the use of nanofluids (Al₂O₃-water) at different concentrations (0%, 2%, 4%, and 6%) to evaluate their synergistic effect with the geometrical modifications. The current study's methods and breadth are innovative since, as far as we know, this integrated approach has never been documented in the literature.

2. NUMERICAL ANALYSES

2.1 Model description

Figure 1 displays a 2-dimensional numerical calculation domain of duct geometry with the double forward-facing step is illustrated schematically. At a distance of 0.2 from the entrance there are 3 rows of circular cylinders with a cross section of 0.02 m diameters.

To ascertain their impact on heat transfer, flow characteristics, and pressure drop, three corrugated surfaces—triangular, sinusoidal, and semicircular—were chosen. employing three distinct volume fractions of the nanoparticles (0%, 2%, 4% and 6%), a turbulent velocity nanofluid (Al₂O₃-water) with a Reynolds number between 15×10^3 and 4×10^4 was selected for this simulation. The figure represents the boundary conditions.

Consequently, the top of the duct is insulated, and the steps are heated and maintained at a steady heat flux (4000w/m²). The first and second steps' heights were maintained at 0.03 meters. The measurements of the channel length and entry width were 1.5 and 0.17 meters, respectively. All duct dimensions are detailed in Table 1. ANSYS-FLUENT software has been utilized to solve flow as well as heat transfer calculations based on the finite volume approach. Thermo-physical properties of the nanofluid displays in Table 2.

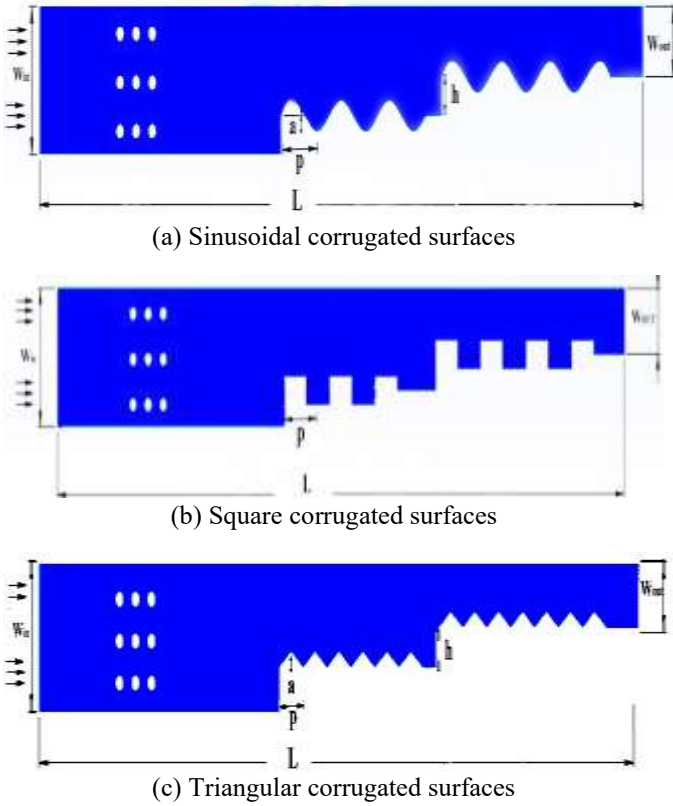


Figure 1. The schematic diagram of the pipe

Table 1. Geometrical parameters for the physical model

Parameter	Symbol	Dimensions
Total length	L	1.5 m
Entrance width	W _{in}	0.17 m
Exit width	W _{ex}	0.1 m
Steps height	h	0.03 m
Corrugated height	a	0.01 m
Corrugated pitch	p	0.04 m
Diameter of the circle	d	0.02 m

Table 2. Thermo-physical properties of base fluid water (H₂O) and solid nanoparticles (Al₂O₃) [26]

Material	ρ (kg/m ³)	C _p (J/kg K)	k (W/m K)
Pure water	997.1	4179	0.613
Al ₂ O ₃	1003	531.8	76.5

The numbers displayed in Table 2 evaluated in this work are computed employing the following formulae. The literature follows the same equation convention [26]. The associated equations reflect density, viscosity, specific energy, and thermal conductivity. Symbols and subscripts are explained in the terminology section. Tables were used to select fixed property values for the fluid mixture's 300 K inlet temperature. The outcomes calculated in Table 2 remain constant while the temperature varies during heat transfer. This is not a problem and can be ignored because the temperature disparity is only 30 K and changes in the values of attributes that relate to the difference in temperature may be ignored.

$$\rho_{nf} = (1 - \varphi) \rho_{bf} + \varphi \rho_p \quad (1)$$

$$(\rho C_p)_{nf} = (1 - \varphi) (\rho C_p)_{pf} + \varphi (\rho C_p)_p \quad (2)$$

$$\mu_{nf} = \mu_{pf} (1 + 2.5 \varphi) \quad (3)$$

2.2 Governing equations

This model ignores the gravity effect and assumes a two-dimensional with incompressible and flow that is turbulent. The following is an expression for the fluid region's continuity, momentum, and energy equations:

Equation of continuity [27]:

$$\frac{\partial u}{\partial x} + \frac{\partial v}{\partial y} = 0 \quad (4)$$

Momentum equation in (x, y-direction) [28]:

$$u \frac{\partial u}{\partial x} + v \frac{\partial u}{\partial y} = -\frac{1}{\rho} \frac{\partial P}{\partial x} + \frac{\partial^2 u}{\partial x^2} + \frac{\partial^2 u}{\partial y^2} \quad (5)$$

$$u \frac{\partial v}{\partial x} + v \frac{\partial v}{\partial y} = -\frac{1}{\rho} \frac{\partial P}{\partial y} + \frac{\partial^2 v}{\partial x^2} + \frac{\partial^2 v}{\partial y^2} \quad (6)$$

Energy equation [29]:

$$u \frac{\partial T}{\partial x} + v \frac{\partial T}{\partial y} = \frac{k}{\rho C_p} \left(\frac{\partial^2 T}{\partial x^2} + \frac{\partial^2 T}{\partial y^2} \right) \quad (7)$$

The classic k- ϵ model, one of those most commonly utilized models, replicates the flow's turbulence. This semi-empirical model consists of two equations: one for turbulent kinetic energy dispersion (ϵ) and another for turbulence kinetic transmission of energy (k).

For turbulent kinetic energy (k) [30]:

$$\rho \left(\frac{\partial}{\partial x} (ku) + \frac{\partial}{\partial y} (kv) \right) = \frac{\partial}{\partial x} \left(\frac{\mu_t}{\sigma_k} \frac{\partial k}{\partial x} \right) + \frac{\partial}{\partial y} \left(\frac{\mu_t}{\sigma_k} \frac{\partial k}{\partial y} \right) + G - \rho \epsilon \quad (8)$$

For energy dissipation rate (ϵ) [30]:

$$\rho \left(\frac{\partial}{\partial x} (\epsilon u) + \frac{\partial}{\partial y} (\epsilon v) \right) = \frac{\partial}{\partial x} \left(\frac{\mu_t}{\sigma_\epsilon} \frac{\partial \epsilon}{\partial x} \right) + \frac{\partial}{\partial y} \left(\frac{\mu_t}{\sigma_\epsilon} \frac{\partial \epsilon}{\partial y} \right) + C_{1\epsilon} \rho \frac{\epsilon}{k} G - C_{1\epsilon} \rho \frac{\epsilon}{k} \quad (9)$$

Up to the heat flux ($q_{\text{convection}}$) is as follows:

$$q_{\text{convection}} = m^o c_p (T_{\text{out}} - T_{\text{in}}) \quad (10)$$

We can obtain (mean heat transfer coefficient) from [31]:

$$h = \frac{q_{\text{conv}}}{(T_w - T_b)} \quad (11)$$

The mean wall temperature (T_w) is determined by [32]:

$$T_w = \frac{1}{n} \sum T_{wn} \quad (12)$$

Also, the mean bulk temperature is obtained by [33]:

$$T_b = \frac{\int_0^L \int_0^H \int_0^W \rho c_p u T dx dy dz}{\int_0^L \int_0^H \int_0^W \rho u dx dy dz} \quad (13)$$

The average Nusselt number [34] is determined by:

$$\text{Nu} = \frac{h D_h}{k} \quad (14)$$

The Darcy Weisbach equation is employing to define the friction factor (f) as [35].

$$f = \frac{\Delta P \cdot D_h}{\frac{1}{2} \rho U_{avg}^2 \cdot L} \tag{15}$$

The overall performance factor (η) [36]:

$$\eta = (Nu/Nu_0)/(f/f_0)^{1/3} \tag{16}$$

2.3 Boundary conditions

The equations are meant to be solved by applying boundary conditions to the boundaries of the numerical domain as in Table 3.

Table 3. The boundary conditions of the simulation

Boundary Ends	Boundary Conditions
Inlet	$T_{in} = 300\text{ K}$, $Re = 10,000\text{-}35,000$
Outlet	$(\partial u/\partial x = \partial v/\partial y = 0)$, zero gauge-pressure is specified at outlet domain
	The velocity is taken to be zero (no slip), $u = 0$, $v = 0$
Surfaces	Heat flux on the corrugated surfaes = 5500 w/m^2 , $\partial P/\partial n = 0$, where n is a normal unit vector

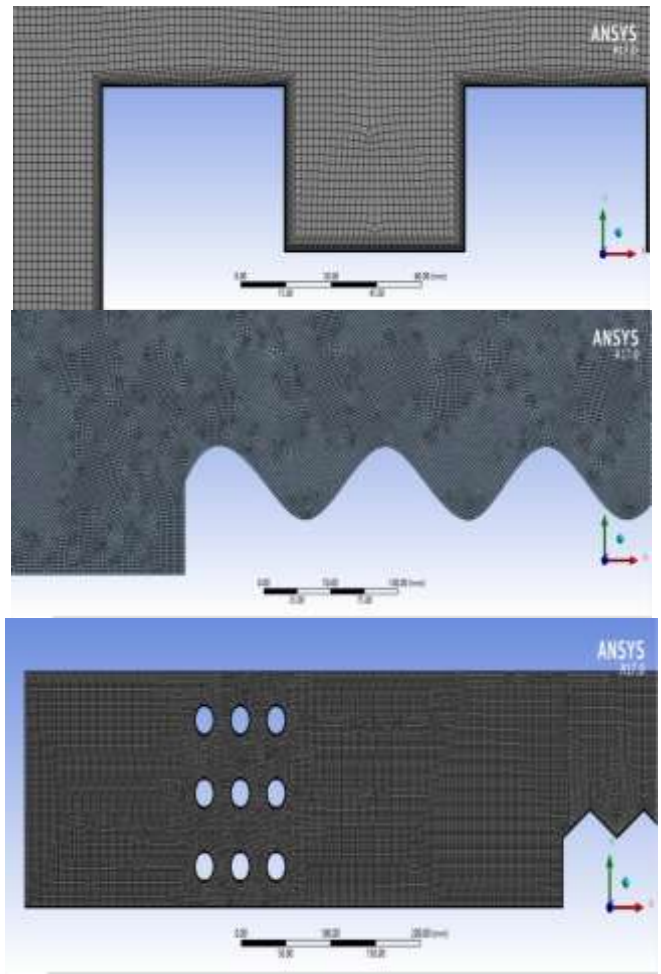


Figure 2. The considered mesh generation

2.4 Mesh generation grid independency

Extensive investigations employing multiple grid densities

for the evaluated Reynolds number were conducted to examine if the projected numerical findings are grid independent. Different uniform mesh densities are utilized to achieve mesh-independent outcomes, and the results are compared until the difference is minimal.

Grid independence was declared using the parameter at the center plane wherein the shear stress equals zero. In CFD Ansys FLUENT 2022, continuity, energy, and momentum are approximated and solved by the application of finite elements. Assuming the $k-\epsilon$ model, the concept of diffusion in the energy and momentum equations was addressed by utilizing the difference between second-order and the up wind. Figure 2 employs a uniform and non-uniform mesh creation technique. For each scenario, the grid independence assessments are performed at $Re = 15 \times 10^3$. The grid independence study is summarized in Table 4 with the most recent four results of the (Nu) and (friction factor) with their total number of elements until the results show the least amount of variation. Grid independence was attained, as evidenced by the less than 1.5% difference between Grids 4 and 5. Additionally, the non-dimensional wall distance y^+ was assessed to guarantee adequate resolution close to the walls, and values were maintained below 1 on all surfaces. This ensures that near-wall temperature and velocity gradients are accurately captured, which is essential for CFD heat transfer studies.

Table 4. Different grids and their (Nu)and(f)for different tested cases at $Re = 15,000$

Case	No. of Grid Elements	Nu	f
Case with smooth surfaces	41,687	62.215	0.0677
	44,722	65.953	0.0733
	48,110	67.521	0.0882
	53,464	69.44	0.0955
	55,448	69.46	0.101
Case with square corrugated surfaces	59,865	117.65	0.08
	61,122	123.75	0.091
	65,612	126.78	0.095
	68,765	128.25	0.104
	73,839	128.34	0.108
Case with triangular corrugated surfaces	47,433		
	52,698	137.21	0.182
	55,624	138.56	0.189
	59,655	140.38	0.2
	63,440	140.54	0.211
Case with sinusoidal corrugated surfaces	42,082	88.54	0.086
	46,114	94.89	0.092
	48,665	95.76	0.096
	51,226	97.88	0.101
	53,622	98.123	0.106

3. RESULTS AND DISCUSSION

A mathematical model of fluid motion in a forward-facing step channel is conducted to assess its performance following the addition and testing of different variables affecting heat transfer and pressure change. Utilizing three types of corrugated walls—square, triangular, and sinusoidal—improves the channel's thermal performance in addition to the arrays of circular clinder cross-section at 0.2 m after the entrance. As well as figure displays the outcomes of the flat surface case to explain clearly the difference between the behavior of the duct with and without corrugated walls. Additionally, one of the extremely conductive nanoparticles

(Al₂O₃) is added to the flowing water. The results are then assessed at several volume fractions (0.0, 0.02, 0.04, and 0.06) to determine which one best improves overall performance.

Figure 3 demonstrate that heat transmission rises with fluid velocity in all cases examined with respect to the Nusselt number. The fluid may absorb more heat from the wall of the channel as its velocity and momentum increase with a higher Re number. This also reduces the temperature differential among the fluid's bulk and channel walls, which in turn raises the Nusselt number.

The effects of introducing three type of corrugated surfaces and employing different value fraction of nanoparticles to the fluid in flow (water) on heat transfer to the fluid, pressure drop, and ultimate thermal-performance have been the topic of numerous studies.

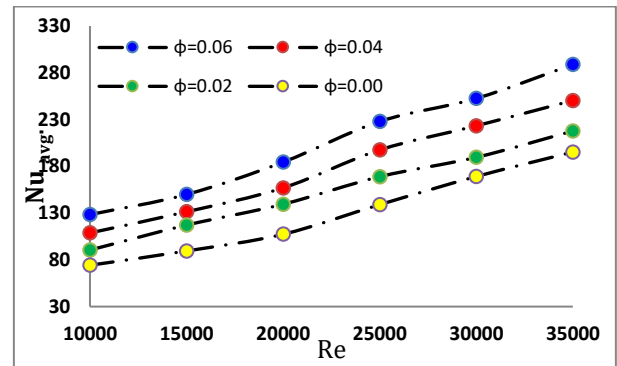
This is especially noticeable when the nanofluid is used with a triangular-shaped corrugated surface, that results in a greater quantity of heat transmission, especially at the maximum volume fraction (0.06). The oblique surfaces of the triangle and the sharp edge can create an extra recirculation area behind the triangular corrugation, which increases the flow's vortex strength and turbulence intensity and forms complex flow, which improves heat transfer. This is the reason why fluid flow rate and heat transfer rate outcomes are rising at the triangular shape. Consequently, we discovered a linear relationship between the rise in the level of nanoparticles in the fluid that flows and the heat transmission. This transfer is strongly influenced by the surface type and form. Sharp edges on triangular corrugated surfaces result in abrupt flow separation, resulting in more mixing and boosts heat transfer. In contrast, square and sinusoidal corrugated surfaces undergo less abrupt separation, which results in weaker turbulence and reduced heat transfer; at sinusoidal, however, the flow keeps more streamlined because there are no sharp edges.

As regard to the circular cylinder, they serve as a convection enhancer, by improve mixing and hence increase heat transmission, the circular cylinders are disrupting the surrounding thermal boundary layers causing rising in heat transfer efficiency and they also create vortices behind each cylinder. In addition, the presence of various rows reduces the temperature gradient along the channel, as heat is redistributed between the different stages of the fluid flow. At increasing flow velocities, enhanced convection heat transfer is projected to cause this trend.

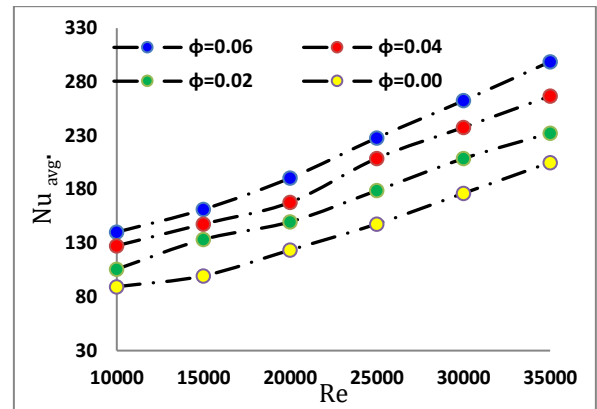
The flow is more stable and shows less mixing close to the heated wall at minimal Re, which leads to less disruption of the thermal boundary layer. Stronger inertial impacts, thinner boundary layers, and more violent heat transfer result from the flow's rising velocity as Re rises. This effect is further enhanced by the presence of nanofluids because of the higher heat conductivity and microscale blending brought on by the movement of nanoparticles. Because of its sharp corners, which accelerate vortex formation and improve local turbulence, the triangular wavy walls exhibits the steepest rise in the Nu with Re among the examined geometries.

Figure 4 illustrates the friction factor in relation to the Re number and particle s volume fraction (0.00, 0.02, 0.04, & 0.06) for three investigated scenarios of the stairs' lower surfaces. When the presence of triangle corrugating is examined in relation to flow direction, it is found to increase the friction factor. at Re = 10,000, the triangle-shaped corrugating increases the friction factor by 1.7 and 2.5 times, in comparison to square and sinusoidal respectively under the same conditions. In the other examples in figures, raising the

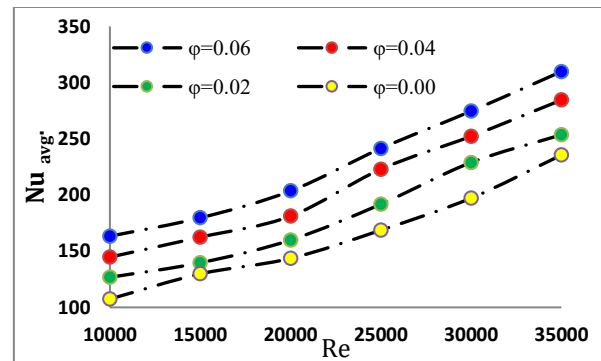
volume of nanoparticles significantly rises the friction factor. Fluid viscosity increases when nanoparticles are present, and the friction factor increases in tandem with the volume fraction of nanoparticles.



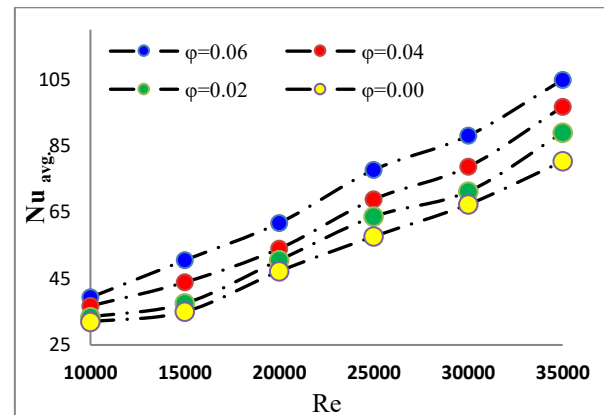
(a) For the case of sinusoidal corrugated surface



(b) For the case of square corrugated surface

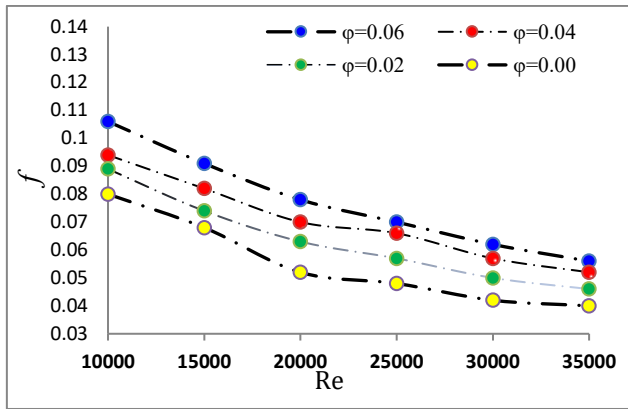


(c) The case of triangular corrugated surface

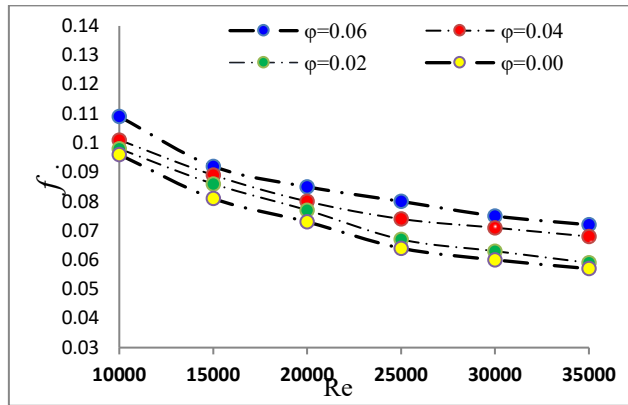


(d) The case of flat surface

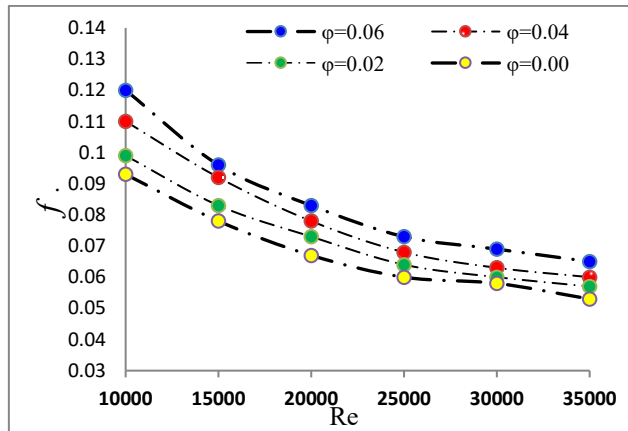
Figure 3. The variation of (Nu) with Re numbers for all tested cases



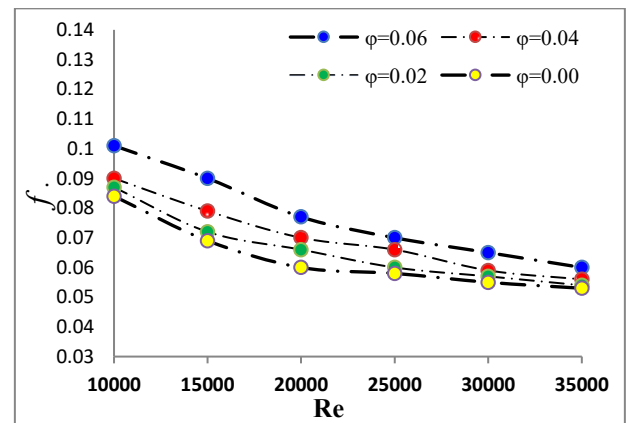
(a) For the case of sinusoidal corrugated surface



(b) For the case of square corrugated surface



(c) The case of triangular corrugated surface



(d) The case of flat surface

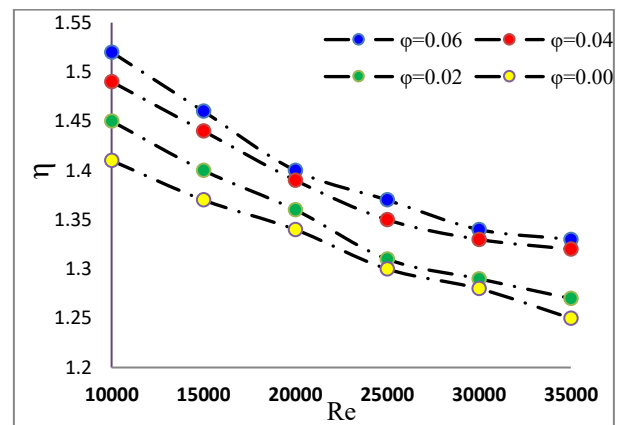
Regarding the reduction of the friction factor as the Re number rises. Because the thinner boundary layer results from a higher Re number, the effects of the viscous area, velocity gradient, shear stress, and friction factor are all minimized. The presence of circular cylinders also leads to higher pressure drop values and thus an increase in the friction factor. The findings reported that the friction factor of triangular friction factor was increased by 11% as compared to square case and 18% as compared to sinusoidal and 26% as compared to the flat surfaces case.

Greater frictional resistance results from viscous processes predominating and the flow adhering more tightly to the wall surfaces at lower Re. A reduced friction factor results from the relative impact of the viscosity decreasing as Re rises and the flow's inertia becoming more dominating. However, because of their improved interaction between surfaces and recirculation zones, geometries with acute corrugations—like the triangle profile—consistently show greater friction factors. A smoother flow pathway with fewer sudden interruptions is suggested by the sinusoidal shape, which has the least frictional resistance of the three.

In Figure 5, the entire performance in each channel has established by analyzing the fluid's behavior, the impact of surface shape, and the addition of nanoparticles to the water. The three figures clearly show a comparison based on nanoparticles and the presence of three different surface in the lower of the step of the channel. The best thermal-compressive performance was demonstrated in the case of triangular, $\eta = 1.76$, and $\phi = 0.06$. Next, the $\phi = 0.04$ case yields $\eta = 1.7$, while the case of $\phi = 0.02$ yields $\eta = 1.64$ and $\eta = 1.57$ in $\phi = 0.00$ case, all at $Re = 10,000$.

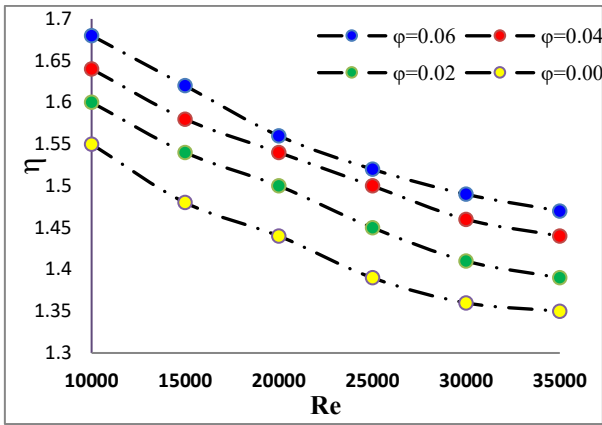
The findings reported that the overall performance of triangular case was increased by 14% as compared to square case and 19% as compared to sinusoidal case. The equilibrium between rising heat transfer and increasing pressure losses causes this behavior. The PEC rises for decreasing Re because the rise in heat transfer is greater than the rise in pumping power.

Frictional losses, however, increase more quickly at very high Re and could cancel out the thermal gains. Throughout the whole range, the triangle-shaped maintains the greatest PEC, demonstrating that its advantage in heat transfer outweighs its higher friction. Because of its smoother, fewer disruptive profile, the sinusoidal shape delivers the least improvement in performance, while the square geometry offers modest performance.

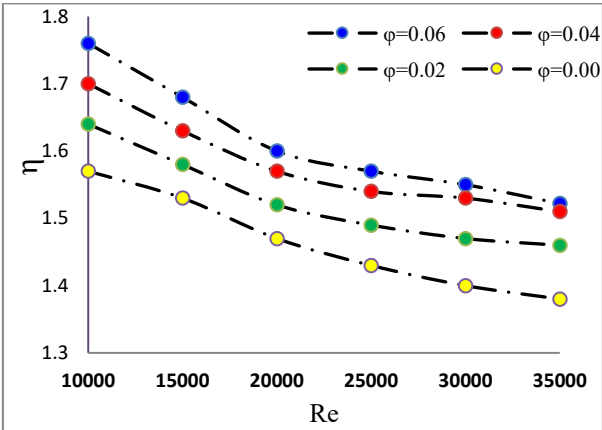


(a) For the case of sinusoidal corrugated surface

Figure 4. The variation of (f) with Re numbers for all tested cases



(b) For the case of square corrugated surface



(c) The case of triangular corrugated surface

Figure 5. The variation of the performance with Re numbers for all tested cases

Hilo et al.'s [37] flow and heat transfer data over the backward-facing step and Hamzah and Tarish's [38] application of a triangular corrugated wall at the lower of the forward-facing step channel with simulated results are compared to validate the algorithm. Figure 6 displays the validation for the fluid turbulent flow over a forward-facing step using the average Nusselt number, which demonstrated good agreement. The difference between the current results and Hilo et al. [37] is 14%, and with Hamzah and Tarish [38] it is 6%.

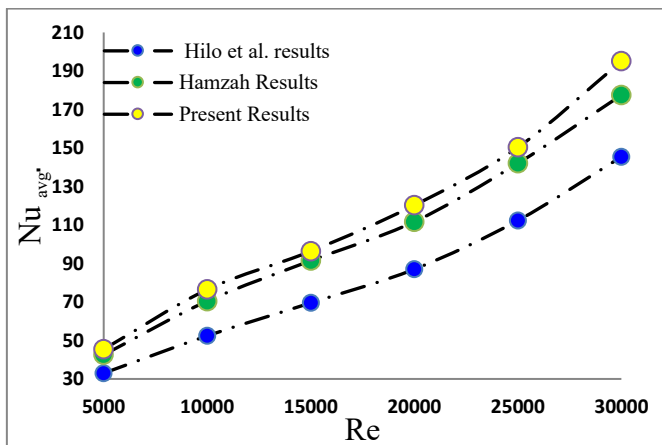
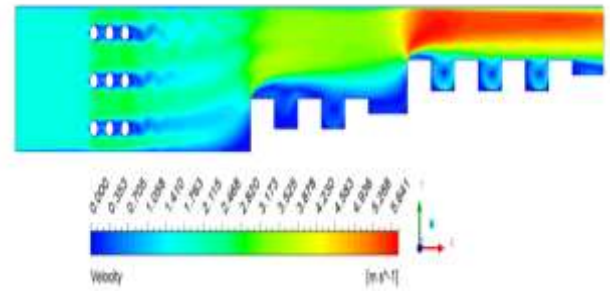


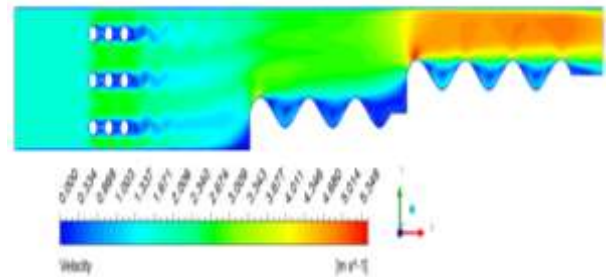
Figure 6. The validation between the present outcomes and Hilo et al. [37] and Hamzah and Tarish [38] results

Generally, following the examination of the velocity

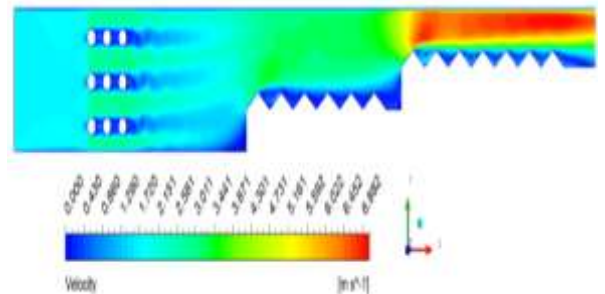
contour at $Re = 10,000$ and $\phi = 0.06$, for all instances the illustrations at Figure 7. Two re-circulation zones have been observed before and after each step, as illustrated by the improvement in the heat transfer rate. The largest turbulent kinetic energy is observed after the second step, which provided a demonstration of achieving thermal performance at this step across all cases. whereas the recirculation area prior to the first and following steps diminishes. In other words, with the increase in flow velocity, the recirculation areas before steps become compressed, whereas those after steps are expanded and enlarged. The turbulent kinetic energy's turbulent flux is illustrated in figure for the triangular corrugated surface case.



(a) Square corrugated surfaces



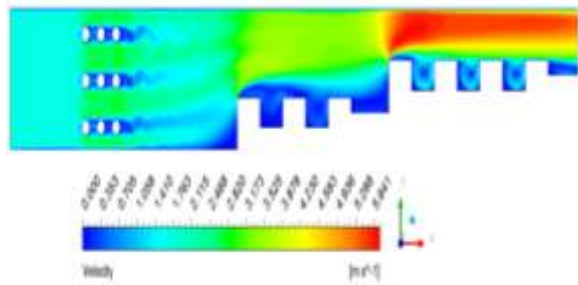
(b) Sinusoidal corrugated surfaces



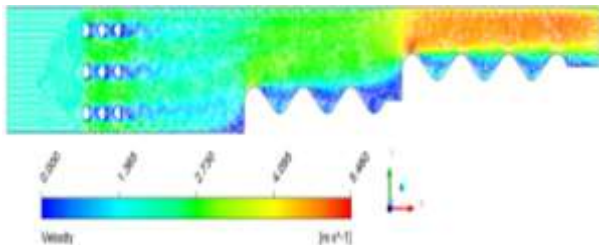
(c) Triangular corrugated surfaces

Figure 7. Velocity contours of the three corrugated cases for $Re = 10,000$, $\phi = 0.06$

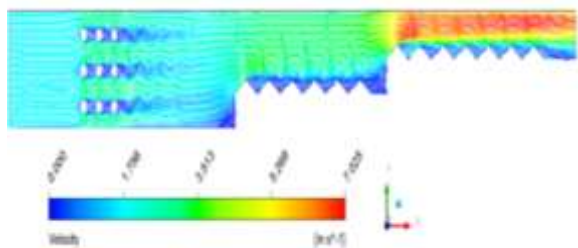
As in Figure 8, as the flow confronts a sudden step, it separates right after the step, resulting in a recirculation zone behind each step. In these areas, the speed of the flow declines considerably or becomes negative, and the flow reorganizes itself with a reattachment region. Regarding the impact of undulating surfaces, elevated regions result in accelerated flow (greater velocity), whereas recessed areas induce deceleration and possibly temporary separation. Regarding circles, they resulting in the flow separating from their front edges. After each circle, a wake region develops. In this wake, the velocity diminishes and persistent vortices emerge. This exacerbates turbulence and makes the flow pattern more complex.



(a) Square corrugated surfaces

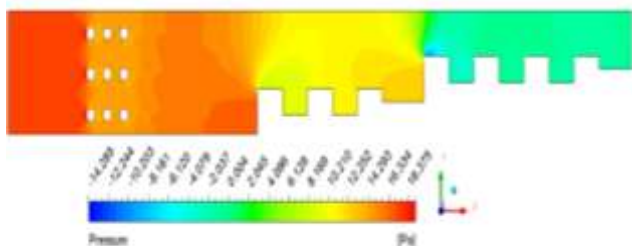


(b) Sinusoidal corrugated surfaces

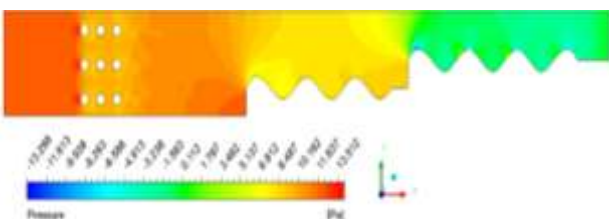


(c) Triangular corrugated surfaces

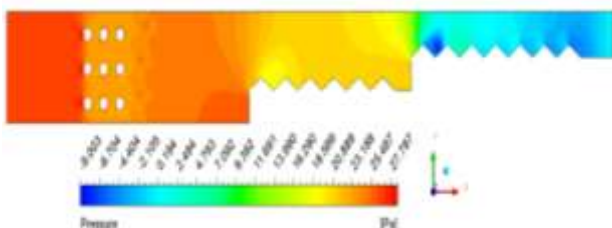
Figure 8. Velocity vectors of the three corrugated cases for $Re = 10000$, $\phi = 0.06$



(a) Square corrugated surfaces



(b) Sinusoidal corrugated surfaces



(c) Triangular corrugated surfaces

Figure 9. Velocity vectors of the three corrugated cases for $Re = 10000$, $\phi = 0.06$

As for Figure 9, after every step, a sudden decrease in pressure takes place as a result of separation, leading to the formation of a very low-pressure zone within the area of the return vortex. Afterwards, as the flow reconnects with the wall, there is a slight gradual heightening in pressure. Throughout the extending of the channel, pressure oscillates periodically at the undulation on the downward surface, decreasing at the crest and rising at the base of each undulation.

4. CONCLUSION

From the simulation conducted for the above cases, we can conclude the following:

1. Adding a corrugating to the lower surfaces exposed to heating significantly raised the amount of heat transferred due to the increased surface area exposed to heating, as well as the generation of larger vortices and thus greater mixing.
2. The presence of circular cylinders contributed to enhancing heat transfer as a result of their obstruction of flow, thus generating greater fluid turbulence, which increased mixing.
3. The results showed that the triangular shape has the advantage in heat transfer, followed by the square, and then the sinusoidal shape. The increase in Nusselt values for the triangular case was 17 and 24 compared to the square and sinusoidal cases respectively, for all nanoparticle concentrations.
4. The amount of improvement in heat transfer compared to flat lower surfaces ranged from 4.77 to 3.62 (from $Re = 10,000$ to 35,000 respectively) for triangular case.
5. Heat transfer, pressure coefficient, and overall channel performance increase with the addition of higher concentrations of nanoparticles. When added, the effective thermal conductivity of the fluid raises and forced convection is improved up to the impact of micro-vortices. As for the raising in friction factor, Nanoparticles rise the dynamic viscosity of the fluid, making the flow more viscous and increasing flow resistance. Thus, it led to a rise in the friction factor.
6. Through the investigations conducted on all cases of this research, the outcomes reported that the maximum performance obtained from triangular corrugated surface at $Re = 10,000$ and with volume fraction of 0.06% ($\eta = 1.76$).

5. RECOMMENDATIONS

1. For better thermal performance, look at hybrid nanofluids or alternative nanoparticle kinds.
2. Expand the study to include unstable and turbulent flow regimes.
3. Examine differences in obstacle spacing and step geometry.
4. Carry out experimental validation and three-dimensional simulations.
5. Examine how the characteristics of the wall material affect the behavior of heat transfer.

REFERENCES

- [1] Podvin, B., Fraigneau, Y. (2024). Low-dimensional

- analysis and modelling of the flow over a forward-facing step. *Journal of Fluid Mechanics*, 1000: A69. <https://doi.org/10.1017/jfm.2024.1051>
- [2] Yashwanth, S., Satheesh, A., Arumugam, S.K., Rajesh Kanna, P., Chidambaram, R.K., Taler, D., Sobota, T., Taler, J. (2024). Numerical investigations of fluid flow and heat transfer in double forward facing step in the presence of a fin. *Numerical Heat Transfer, Part A: Applications*, 1-23. <https://doi.org/10.1080/10407782.2024.2359051>
 - [3] Hamood, H.M., Mansour, M.M., Lafta, A.M., Nashee, S.R. (2024). Numerical investigation to study the effect of three height of triangular obstacles on heat transfer of nanofluids in a microchannel. *International Review of Mechanical Engineering (IREME)*, 17(11). <https://doi.org/10.15866/ireme.v17i11.23627>
 - [4] Nashee, S., Mushatet, K. (2024). Performance study on turbulent heat transfer using rectangular air duct integrated with continuous and intermittent ribs turbulators. *Thermal Science*, 29(2A): 955-967.
 - [5] Mansour, M.M., Hamood, H.M., Lafta, A.M., Nashee, S.R., Shkarah, A.J. (2024). Enhancing the efficacy of adsorption-based carbon storage systems: A finite element analysis approach. *International Journal of Energy Production and Management*, 9(1): 19-24. <https://doi.org/10.18280/ijepm.090103>
 - [6] Mohammed, K.A., Abu Talib, A.R., Nuraini, A.A., Ahmed, K.A. (2017). Review of forced convection nanofluids through corrugated facing step. *Renewable and Sustainable Energy Reviews*, 75: 234-241. <https://doi.org/10.1016/j.rser.2016.10.067>
 - [7] Mohammed, H.A., Al-Aswadi, A.A., Shuaib, N.H., Saidur, R. (2011). Convective heat transfer and fluid flow study over a step using nanofluids: A review. *Renewable and Sustainable Energy Reviews*, 15(6): 2921-2939. <https://doi.org/10.1016/j.rser.2011.02.019>
 - [8] Nashee, S.R. (2023). Numerical study for fluid flow and heat transfer characteristics in a corrugating channel. *International Journal of Heat and Technology*, 41(2): 392-398. <https://doi.org/10.18280/ijht.410213>
 - [9] Mohammed, H.A., Alawi, O.A., Wahid, M.A. (2015). Mixed convective nanofluid flow in a channel having backward-facing step with a baffle. *Powder Technology*, 275: 329-343. <https://doi.org/10.1016/j.powtec.2014.09.046>
 - [10] Togun, H. (2016). Laminar CuO–water nano-fluid flow and heat transfer in a backward-facing step with and without obstacle. *Applied Nanoscience*, 6: 371-378. <https://doi.org/10.1007/s13204-015-0441-7>
 - [11] Nashee, S.R. (2024). Enhancement of heat transfer in nanofluid flow through elbows with varied cross-sections: A computational study. *International Journal of Heat and Technology*, 42(1): 311-319. <https://doi.org/10.18280/ijht.420133>
 - [12] Rahman, M.A. (2024). Thermo-fluid performance of axially perforated multiple rectangular flow deflector-type baffle plate in a tubular heat exchanger. *Applications in Engineering Science*, 20: 100197. <https://doi.org/10.1016/j.apples.2024.100197>
 - [13] Fang, X.J., Tachie, M.F., Bergstrom, D.J. (2021). Direct numerical simulation of turbulent flow separation induced by a forward-facing step. *International Journal of Heat and Fluid Flow*, 87: 108753. <https://doi.org/10.1016/j.ijheatfluidflow.2020.108753>
 - [14] Iftekhhar, H., Agelin-Chaab, M. (2016). Structure of turbulent flows over forward facing steps with adverse pressure gradient. *Journal of Fluids Engineering*, 138(11): 111202. <https://doi.org/10.1115/1.4033030>
 - [15] Shao, W.J., Agelin-Chaab, M. (2016). Turbulent flows over forward facing steps with surface roughness. *Journal of Fluids Engineering*, 138(2): 021103. <https://doi.org/10.1115/1.4031258>
 - [16] He, W., Toghraie, D., Lotfipour, A., Pourfattah, F., Karimipour, A., Afrand, M. (2020). Effect of twisted-tape inserts and nanofluid on flow field and heat transfer characteristics in a tube. *International Communications in Heat and Mass Transfer*, 110: 104440. <https://doi.org/10.1016/j.icheatmasstransfer.2019.104440>
 - [17] Barkley, D., Gomes, M.G.M., Henderson, R.D. (2002). Three-dimensional instability in flow over a backward-facing step. *Journal of Fluid Mechanics*, 473: 167-190. <https://doi.org/10.1017/S002211200200232X>
 - [18] Kherbeet, A.S., Mohammed, H.A., Salman, B.H., Ahmed, H.E., Alawi, O.A., Rashidi, M.M. (2015). Experimental study of nanofluid flow and heat transfer over microscale backward-and forward-facing steps. *Experimental Thermal and Fluid Science*, 65: 13-21. <https://doi.org/10.1016/j.expthermflusci.2015.02.023>
 - [19] Kherbeet, A.S., Mohammed, H.A., Munisamy, K.M., Salman, B.H. (2014). Combined convection nanofluid flow and heat transfer over microscale forward-facing step. *International Journal of Nanoparticles*, 7(1): 1-25. <https://doi.org/10.1504/IJNP.2014.062008>
 - [20] Abu-Nada, E. (2008). Application of nanofluids for heat transfer enhancement of separated flows encountered in a backward facing step. *International Journal of Heat and Fluid Flow*, 29(1): 242-249. <https://doi.org/10.1016/j.ijheatfluidflow.2007.07.001>
 - [21] Christopher, D.S., Madhusudhana, G.R., Venkumar, P., Kanna, P.R., Mohammed, H.A. (2012). Numerical investigation on laminar flow due to sudden expansion using nanofluid. *Journal of Computational and Theoretical Nanoscience*, 9(12): 2217-2227. <https://doi.org/10.1166/jctn.2012.2642>
 - [22] Kanna, P.R., Das, M.K. (2006). Heat transfer study of two-dimensional laminar incompressible wall jet over backward-facing step. *Numerical Heat Transfer, Part A: Applications*, 50(2): 165-187. <https://doi.org/10.1080/10407780500506857>
 - [23] Nie, J.H., Armaly, B.F. (2004). Reverse flow regions in three-dimensional backward-facing step flow. *International Journal of Heat and Mass Transfer*, 47(22): 4713-4720. <https://doi.org/10.1016/j.ijheatmasstransfer.2004.05.027>
 - [24] Sherry, M., Lo Jacono, D., Sheridan, J. (2010). An experimental investigation of the recirculation zone formed downstream of a forward facing step. *Journal of Wind Engineering and Industrial Aerodynamics*, 98(12): 888-894. <https://doi.org/10.1016/j.jweia.2010.09.003>
 - [25] Li, Z.Y., Guo, S., Bai, H.L., Gao, N. (2019). Combined flow and heat transfer measurements of backward facing step flows under periodic perturbation. *International Journal of Heat and Mass Transfer*, 130: 240-251. <https://doi.org/10.1016/j.ijheatmasstransfer.2018.10.077>
 - [26] Mohammed, H.A., Hussein, O.A. (2014). Assisting and opposing combined convective heat transfer and nanofluids flows over a vertical forward facing step.

- Journal of Nanotechnology in Engineering and Medicine, 5(1): 010903. <https://doi.org/10.1115/1.4028009>
- [27] Abdulkarim, A.H., Eleiwi, M.A., Tahseen, T.A., Canli, E. (2021). Numerical forced convection heat transfer of nanofluids over back facing step and through heated circular grooves. *Mathematical Modelling of Engineering Problems*, 8(4): 597-610. <https://doi.org/10.18280/mmep.080413>
- [28] Nashee, S.R., Mushatet, K.S. (2025). Impact of ribs with multiple arrangements on the behavior of a turbulent flow in a rectangular channel. *Journal of Heat and Mass Transfer Research*, 12(2): 259-270. <https://doi.org/10.22075/jhmtr.2025.34713.1575>
- [29] Rahman, A. (2023). Experimental investigations on single-phase heat transfer enhancement in an air-to-water heat exchanger with rectangular perforated flow deflector baffle plate. *International Journal of Thermodynamics*, 26(4): 31-39. <https://doi.org/10.5541/ijot.1285385>
- [30] Nashee, S.R. (2024). Numerical simulation of heat transfer enhancement of a heat exchanger tube fitted with single and double-cut twisted tapes. *International Journal of Heat and Technology*, 42(3): 1003-1010. <https://doi.org/10.18280/ijht.420327>
- [31] Shakir, R. (2022). Study of pressure drop and heat transfer characteristics of mini-channel heat sinks. *The Iraqi Journal for Mechanical and Materials Engineering*, 22(2): 85-97. <https://doi.org/10.32852/ijqfmme.v22i2.595>
- [32] Rahman, A., Dhiman, S.K. (2024). Thermo-fluid performance of a heat exchanger with a novel perforated flow deflector type conical baffles. *Journal of Thermal Engineering*, 10(4): 868-879. <https://doi.org/10.14744/thermal.0000846>
- [33] Nashee, S.R., Ibrahim, Z.A., Kamil, D.J. (2024). Numerical investigation of flow in vertical rectangular channels equipped with three different obstacles shape. *AIP Conference Proceeding*, 3122: 100002. <https://doi.org/10.1063/5.0216016>
- [34] Abdul Razzaq, A.K., Mushatet, K.S. (2021). A numerical study for a double twisted tube heat exchanger. *International Journal of Heat and Technology*, 39(5): 1583-1589. <https://doi.org/10.18280/ijht.390521>
- [35] Nashee, S.R., Mansour, M.M., Salman, H.S., Lafta, A.M. (2025). Investigation of the optimum shape of the fins for maximum heat dissipation. *AIP Conference Proceedings*, 3303(1): 060012. <https://doi.org/10.1063/5.0263011>
- [36] Mushatet, K.S., Bader, N.M. (2022). Experimental investigation for the performance of the solar air dryer with vortex generator. *Defect and Diffusion Forum*, 419: 57-67. <https://doi.org/10.4028/p-a8x5o3>
- [37] Hilo, A.K., Talib, A.R.A., Iborra, A.A., Sultan, M.T.H., Hamid, M.F.A. (2020). Effect of corrugated wall combined with backward-facing step channel on fluid flow and heat transfer. *Energy*, 190: 116294. <https://doi.org/10.1016/j.energy.2019.116294>
- [38] Hamzah, M.T., Tarish, A.L. (2020). Numerical study of the effect of corrugated wall on the turbulent forced convective heat transfer and fluid flow through a forward-facing step channel. *Journal of Advanced Research in Fluid Mechanics and Thermal Sciences*, 67(1): 33-42.

NOMENCLATURE

A	surface area, m ²
a	Amplitude of the corrugation, m
D _h	hydraulic-diameter, m
f	friction, factor
h	mean heat, transfer coefficient, W/m ² K
h _{1,h2}	height of steps, m
k	thermal conductivity, W.m ⁻¹ . K ⁻¹
L	length of duct, m
Nu _L	local Nusselt number along the heat source
Nu	mean Nusselt number
p	pitch of corrugation, m
Δp	pressure-drop of channel, pa
q _{conv}	the convective heat flux, W/m ²
Re	Reynolds number
T _w	wall. temperature, K
T _{in}	inlet temperature, K
T _{out}	outlet temperature, K
T _b	bulk temperature, K

Greek symbols

η	overall performance
ρ	density
μ	dynamic viscosity, kg. m ⁻¹ .s ⁻¹